Output Phase and Amplitude Analysis of GaN-Based HEMT at Cryogenic Temperatures

Haowen Guo, Junmin Zhou, Maojun Wang, *Member, IEEE*, and Xinbo Zou, *Member, IEEE*

***Abstract*— We report both output phase and amplitude performance for gallium nitride (GaN)-based high-electron-mobility transistor (HEMT), operating in RF small- and large-signal modes from 270 K to cryogenic 70 K. Intrinsic elements of the device were extracted employing a small-signal equivalent circuit model. Temperature dependences of maximum available power gain, short-circuit current gain, and open-circuit voltage gain indicated performance improvement as lowering the ambient temperature. Meanwhile, the output phase of small RF signal measurement was found to be decreased linearly with decreasing the temperature. In RF large-signal operations, power and phase nonlinearity induced by AM-to-AM and AM-to-PM conversion were characterized via gain and phase compression, respectively. Measured $P_{1\,dB}/P_{3\,dB}/P_{5\,dB}$ was decreased monotonously for $T > 150$ K, whereas it showed little temperature sensitivity under 150 K. Output phase shift was expanded as increasing the input power level and was all greatly suppressed as dropping the temperature.**

***Index Terms*— Amplitude compression, cryogenic temperature, gallium nitride (GaN), high-electron-mobility transistor (HEMT), phase compression.**

I. Introduction

AlGaN/GALLIUM nitride (GaN)-based high-electron-mobility transistors (HEMTs) have emerged as promising candidates for high-frequency applications such as wireless communication, radar sensing, and high-resolution positioning, due to the large carrier mobility and substantial drain current [1]–[3]. Due to outstanding thermal stability, GaN HEMTs enable operations over a wide temperature range. There have been some investigations studying temperature impact on the frequency performance of GaN-based HEMTs [4]–[7]. Most of them were devoted to measurements and discussions at or above room temperature. However, there is a lack of data available for cryogenic environments, which is important for applications, including space exploration and satellite communications. When evaluating modulated signal quality, e.g., performing measurements of error vector magnitude (EVM) in high-order modulation transmitter system and signal-to-noise ratio in phased-array receiver, phase analysis is equally important as the amplitude or power degradation study [8], [9]. Currently, there are a few reports about temperature-dependent phase shift in either small- or large-signal operations of GaN HEMTs.

In this letter, the temperature impact on RF small- and large-signal operations was studied for GaN HEMT on Si, which is promising to achieve high performance with much reduced cost. S_{21} phase in small-signal mode was utilized to analyze the phase behavior as a function of temperature. In addition to the linear region study, the nonlinear distortions induced by amplitude-to-amplitude conversion (AM-to-AM) and amplitude-to-phase conversion (AM-to-PM) were revealed via gain and phase compression measurements, respectively [10], [11]. Different from the commonly used two-tone intermodulation method, a compression measurement method was employed in this work, due to the fact that it can well characterize both the amplitude and the phase performance. However, two-tone intermodulation typically only provides the amplitude information with third-order intercept point (IP3) or intermodulation distortion (IMD). Study on nonlinear amplitude and phase properties in cryogenic environments as well as their temperature dependence paved a solid pathway for designing reliable monolithic microwave integrated circuit (MMICs) functioning properly in extreme temperatures and large-signal conditions.

II. Experimental Methods

The HEMT on Si epilayer was provided by NTT-AT, and from bottom to top, it consists of a nucleation layer, 4-μm-thick C-doped buffer layer, 300-nm undoped channel layer, and 30-nm undoped $Al_{0.25}Ga_{0.75}N$ barrier layer. The device used Ti/Al/Ni/Au (20/160/50/100 nm) as ohmic contact after mesa isolation. A 150-nm-thick Si_3N_4 layer was deposited by plasma-enhanced chemical vapor deposition (PECVD) at 300 °C and then annealed for 10 min in N_2 at 400 °C. Then, reactive-ion etching (RIE) gate opening was implemented for Ni/Au gate metal deposition and interconnection. The gate terminal was fabricated into a rectangular shape with a length/width of 1 and 100 μm, respectively.

Based on the scattering parameters (S-parameters) measurement results with RF small signal, device elements were extracted from 270 to 70 K with a temperature step of 10 K, employing the equivalent circuit model shown in Fig. 1(a) [6], [12]. Parasitic capacitances were deembedded using an open-circuit pattern. Given fixed quiescent operating point ($V_{gs} = -3.6$ V and $V_{ds} = 4$ V), elements, including

Manuscript received April 19, 2021; accepted April 30, 2021. Date of publication May 11, 2021; date of current version November 8, 2021. This work was supported in part by the ShanghaiTech University Startup Fund and sponsored by Shanghai Pujiang Program under Grant 18PJ1408200, in part by the Shanghai Eastern Scholar (Youth) Program, and in part by the Chinese Academy of Sciences (CAS) Strategic Science and Technology Program under Grant XDA18000000. *(Corresponding authors: Xinbo Zou; Maojun Wang.)*

Haowen Guo, Junmin Zhou, and Xinbo Zou are with the School of Information Science and Technology (SIST), ShanghaiTech University, Shanghai 201210, China (e-mail: zouxb@shanghaitech.edu.cn).

Maojun Wang is with the Institute of Microelectronics, Peking University, Beijing 100871, China (e-mail: mjwang@pku.edu.cn).

Color versions of one or more figures in this letter are available at https://doi.org/10.1109/LMWC.2021.3079222.

Digital Object Identifier 10.1109/LMWC.2021.3079222

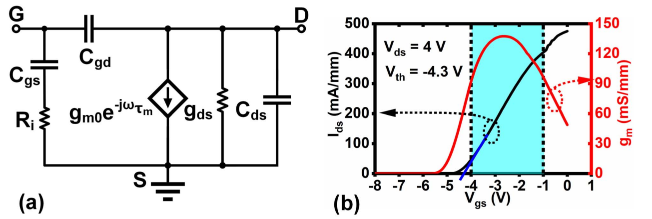

Fig. 1. (a) Small-signal equivalent circuit for GaN HEMT. (b) Transfer and transconductance characteristics at drain bias $V_{ds} = 4$ V at 300 K.

g_{m0}, g_{ds}, C_{gs}, C_{gd}, C_{ds}, R_i, and τ_m, and their temperature dependences were investigated at 2.1 GHz, a frequency extensively used in the wireless communication system. Simulation with advanced design system (ADS) [6] was used to verify the representation of extracted elements of the GaN HEMT. The temperature impact on the output phase was measured in the linear region with input power (P_{in}) of −20 dBm.

Compression measurements were performed to characterize the nonlinearity of GaN HEMT under Class-AB bias condition with RF large signal. The amplitude and phase of transmission performances were evaluated using linear region values as baseline points [13]. Specifically, the reference values of both gain and phase were acquired with P_{in} of −20 dBm.

III. Results and Discussion

A. Amplitude and Phase Behavior in Small-Signal Operations

Fig. 1(b) shows the transfer and transconductance characteristics of the GaN HEMT at room temperature, with $V_{ds} = 4$ V. The threshold voltage V_{th} was determined to be −4.3 V, which was extracted from the linear extrapolation of I_{ds}–V_{gs} curve. In this work, V_{gs} was kept at −3.6 V, around which dc transconductance g_m and the magnitude of S_{21} reached their maximum values. The output characteristic at $V_{gs} = -3.6$ V presents a knee voltage of 1.2 V and a saturation current of 92.4 mA/mm. A breakdown voltage of more than 100 V is achieved in the OFF-state measurement.

Fig. 2 shows the extracted elements from a small-signal equivalent circuit model and time constant τ_{gs} ($\tau_{gs} = R_i \times C_{gs}$) [5]. Temperature-dependent transconductance g_{m0} and output conductance g_{ds} are shown in Fig. 2(a). As decreasing the temperature, g_{m0} was typically increased until 120 K and then slightly dropped, whereas g_{ds} was decreased and then saturated. The evolution of g_{m0} was highly associated with electron mobility–temperature relationship that carrier mobility hits its maximum value at around 120 K. The small g_{ds}, corresponding to the large output resistance, is highly demanded in achieving small power dissipation inside the transistor and higher output microwave power [6]. As shown in Fig. 2(b), the input capacitance C_{gs} is much larger than the other two capacitances. From 270 to 70 K, the increase of C_{gs} would play a negative role in achieving high current gain cutoff frequency (f_T) according to the expression of $g_{m0}/(2\pi \times (C_{gs} + C_{gd}))$. Meanwhile, a reduction of feedback capacitance C_{gd} from 24.4 to 10.7 fF would lead to a high voltage gain and compensate for phase distortion resulted

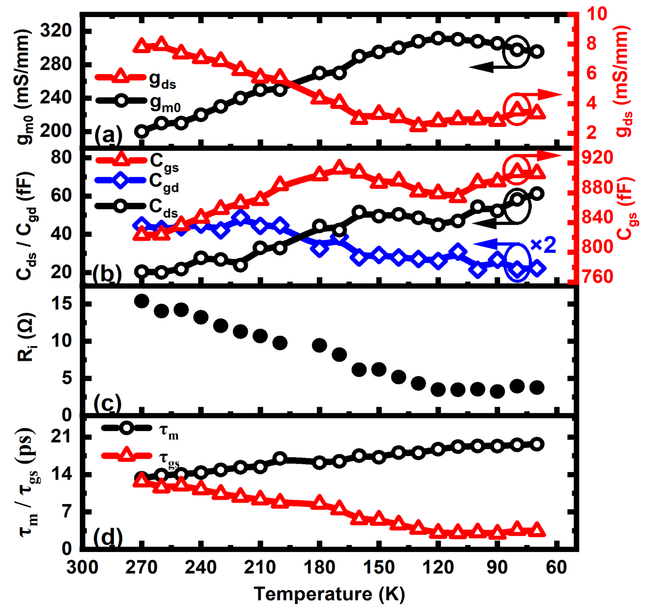

Fig. 2. (a) Transconductances (g_{m0} and g_{ds}). (b) Capacitances (C_{gs}, C_{gd}, and C_{ds}). (c) Resistance (R_i). (d) Time constants (τ_m and τ_{gs}) as a function of temperature.

from g_{m0} nonlinearity [14]. The increased output capacitance C_{ds} as lowering the temperature should be considered and compensated by the susceptance when designing HEMT-based circuits, although C_{ds} has a minor effect on f_T. The measured values of input resistance R_i were reduced from 154 to 32 Ω/mm, as decreasing the temperature [Fig. 2(c)], a trend in a good agreement with the published work [6]. Due to the significant reduction of R_i, the calculated τ_{gs} shows a negative trend with temperature, as shown in Fig. 2(d). The intrinsic delay time τ_m was slightly increased, which was attributed to the increase of depletion length toward the drain terminal, as reflected by the reduction of C_{gd}. Based on linear temperature dependence, it is expressed as: $P(T) = P(T_0)[1+\beta(T - T_0)]$, where $T_0 = 270$ K and β is the temperature coefficient [6], [7]. β of g_{m0}, g_{ds}, C_{gs}, C_{gd}, C_{ds}, R_i, and τ_m is extracted to be −0.38%, 0.51%, −0.11%, 0.3%, −0.98%, 0.5%, and −0.25%, respectively.

Fig. 3(a) reports the maximum available power gain (MAG), short-circuit current gain ($|h_{21}|^2$), and open-circuit voltage gain (A_v). MAG and $|h_{21}|^2$ are derived directly from the measured S-parameters, whereas A_v is derived by g_{m0}/g_{ds}. Due to the small value of g_{ds}, A_v reached its peak value of 124.8 at 130 K, more than doubled than the value obtained at room temperature and those reported in the literature [5]. Both MAG and $|h_{21}|^2$ were typically increased as cooling the environment, and the values were slightly decreased after hitting the peaks at 120 K, 11.4, and 8.5 dB. The slight drop of MAG, $|h_{21}|^2$, and A_v was also attributed to the reduction of electron mobility in the corresponding temperature range, from 120 to 70 K. As shown in Fig. 3(b), both current gain cutoff frequency f_T and maximum work frequency f_{max} were improved, from 3.6 to 4.7 GHz (30.5% improvement) and from 7.1 to 8.6 GHz (21.1% improvement), respectively, although C_{gs} was expanded with decreasing temperature [Fig. 2(b)]. It is attributed to the fact that g_{m0} dictates the variations of

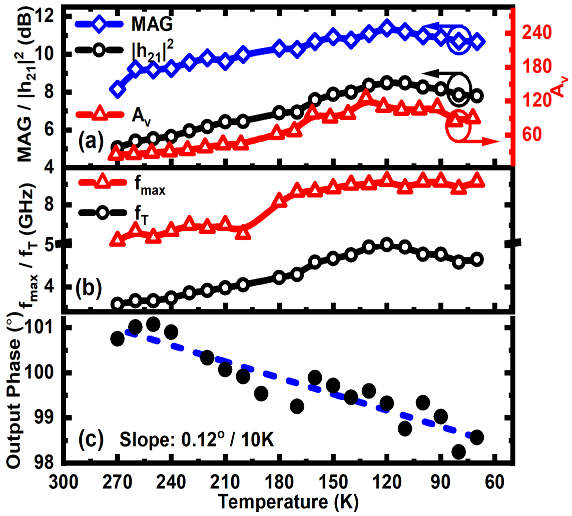

Fig. 3. (a) MAG, $|h_{21}|^2$, and A_v. (b) f_T and f_{max}. (c) Output phase as a function of temperature from 270 to 70 K.

f_T and f_{max} with temperature. f_T and f_{max} could be further improved by shrinking the gate length dimension, as suggested by a number of reports in the literature [15]–[17]. As shown in Fig. 3(c), the measured output phase as a function of temperature could be well fitted by a linear relationship, where a slope of 0.12° per 10 K was obtained. The maximum phase variation for the complete measurement temperature range can be 3°, a potential hazard to the high-performance phased-array receiver front end, where phase error was typically lower than 1° [9].

B. Amplitude and Phase Behavior in Large-Signal Operations

Fig. 4(a) shows that at 200 K, $P_{1\,dB}$, at which 1-dB AM-to-AM compression occurred, was measured to be −8.87 dBm for operation frequency of 2.1 GHz. Fig. 4(b) shows that at 200 K, the phase compression (AM-to-PM conversion) was determined to be 0.82° at P_{in} of 5 dBm.

As shown in Fig. 4(c), the temperature impact on the power nonlinearity (AM-to-AM conversion) is characterized by 1-/3-/5-dB power compression point ($P_{1\,dB}/P_{3\,dB}/P_{5\,dB}$), referring to the input power at which the gain shifts from linearity by 1/3/5 dB. All of the measured $P_{1\,dB}/P_{3\,dB}/P_{5\,dB}$ were decreased monotonously for $T > 150$ K, at which the measured $P_{1\,dB}$ was deviated from its 270 K-point by 1.36 dB and, however, shows little sensitivity to temperatures below 150 K. The assumption [7] that power compression requires a preset output power to reach certain amplitude degradation could explain the lowering of 1-dB points, in a line with the results that higher gain and larger g_{m0} was achieved as decreasing the temperature. Single-tone harmonics were measured at a frequency of 4.2/6.3 GHz with input power of 8 dBm, and the device is biased at the same dc point as the gain and phase compression test ($V_{gs} = -3.6$ V, $V_{ds} = 4$ V). As shown in the inset of Fig. 4(c), the second-/third-order harmonics climb from −27.5/−43.2 to −16.8/−31 dBm as decreasing the temperature. The increasement of harmonics is associated with the lowering of the 1-/3-/5-dB gain compression occurrence,

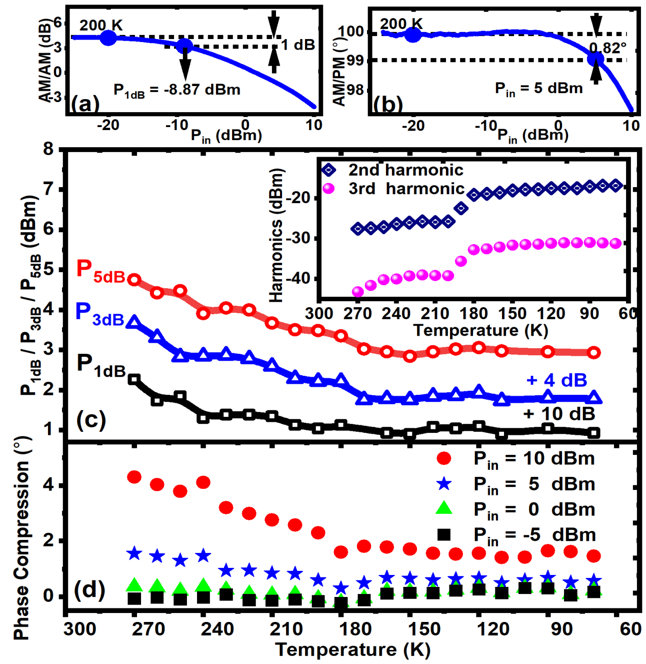

Fig. 4. (a) 1-dB compression point $P_{1\,dB}$. (b) Phase compression at 200 K. (c) 1-/3-/5-dB power compression point. (d) Phase compression with $P_{in} = -5/0/5/10$ dBm as a function of temperature.

which indicates a smaller dynamic range of input RF power at a low or cryogenic temperature.

Fig. 4(d) shows the phase deviations from the reference value, for four different values of P_{in} (−5/0/5/10 dBm). The output phase was typically unchanged as the device was fed with small input power no larger than 0 dBm. However, with a relatively large input power of 10 dBm, the phase compression was decreased from 4.3° at 270 K to 1.6° at 140 K, a temperature dependence that should be considered when designing high-performance millimeter-wave modulators demanding low-EVM. The narrowed and stabilized output phase shift under 150 K was attributed to the reduction of C_{gd} at cryogenic temperatures that phase distortion was reportedly mitigated as suppression of feedback capacitance C_{gd} [14].

IV. Conclusion

The output phase and amplitude of GaN HEMT was investigated from 270 to 70 K, for both RF small- and large-signal operations. Based on small-signal measurements, temperature-dependent amplitude analysis showed that output gains, including MAG, $|h_{21}|^2$, and A_V, were all increased until 120 K and then slightly compromised, while the output phase exhibited a linear decrease for the whole temperature range. Meanwhile, the nonlinearity of large-signal performance was investigated employing gain and phase compression measurements. The 1-/3-/5-dB compressions were found to be occurred at a relatively smaller input power as dropping the temperature until 150 K and showed little temperature sensitivity below 150 K. The phase compression at the input power of 5 dBm or above was typically narrowed down as cooling the environment into cryogenic range. The compression measurement method and results paved a way for characterizations of power and phase nonlinearity of HEMT devices and utilization of GaN-HEMTs for cryogenic RF applications.

REFERENCES

[1] G. Lv, W. Chen, X. Liu, and Z. Feng, "A dual-band GaN MMIC power amplifier with hybrid operating modes for 5G application," *IEEE Microw. Wireless Compon. Lett.*, vol. 29, no. 3, pp. 228–230, Mar. 2019.

[2] R. S. Pengelly, S. M. Wood, J. W. Milligan, S. T. Sheppard, and W. L. Pribble, "A review of GaN on SiC high electron-mobility power transistors and MMICs," *IEEE Trans. Microw. Theory Techn.*, vol. 60, no. 6, pp. 1764–1783, Jun. 2012.

[3] D. Resca, A. Raffo, S. Di Falco, F. Scappaviva, V. Vadala, and G. Vannini, "X-band GaN power amplifier for future generation SAR systems," *IEEE Microw. Wireless Compon. Lett.*, vol. 24, no. 4, pp. 266–268, Apr. 2014.

[4] M. A. Alim, M. A. Hasan, A. A. Rezazadeh, C. Gaquiere, and G. Crupi, "Multibias and temperature dependence of the current-gain peak in GaN HEMT," *Int. J. RF Microw. Comput.-Aided Eng.*, vol. 30, no. 4, Apr. 2020, Art. no. e22129.

[5] G. Crupi, A. Raffo, G. Avolio, D. M. M.-P. Schreurs, G. Vannini, and A. Caddemi, "Temperature influence on GaN HEMT equivalent circuit," *IEEE Microw. Wireless Compon. Lett.*, vol. 26, no. 10, pp. 813–815, Oct. 2016.

[6] M. A. Alim, A. A. Rezazadeh, and C. Gaquiere, "Temperature effect on DC and equivalent circuit parameters of 0.15-μm gate length GaN/SiC HEMT for microwave applications," *IEEE Trans. Microw. Theory Techn.*, vol. 64, no. 11, pp. 3483–3491, Nov. 2016.

[7] A. M. Darwish, B. D. Huebschman, E. Viveiros, and H. A. Hung, "Dependence of GaN HEMT millimeter-wave performance on temperature," *IEEE Trans. Microw. Theory Techn.*, vol. 57, no. 12, pp. 3205–3211, Dec. 2009.

[8] A. K. Gupta and J. F. Buckwalter, "Linearity considerations for low-EVM, millimeter-wave direct-conversion modulators," *IEEE Trans. Microw. Theory Techn.*, vol. 60, no. 10, pp. 3272–3285, Oct. 2012.

[9] R. Garg and A. S. Natarajan, "A-28 GHz low-power phased-array receiver front-end with 360° RTPS phase shift range," *IEEE Trans. Microw. Theory Techn.*, vol. 65, no. 11, pp. 4703–4714, Nov. 2017.

[10] L. C. Nunes, P. M. Cabral, and J. C. Pedro, "AM/AM and AM/PM distortion generation mechanisms in Si LDMOS and GaN HEMT based RF power amplifiers," *IEEE Trans. Microw. Theory Techn.*, vol. 62, no. 4, pp. 799–809, Apr. 2014.

[11] S. Kulkarni and P. Reynaert, "A 60-GHz power amplifier with AM–PM distortion cancellation in 40-nm CMOS," *IEEE Trans. Microw. Theory Techn.*, vol. 64, no. 7, pp. 2284–2291, Jul. 2016.

[12] M. Berroth and R. Bosch, "Broad-band determination of the FET small-signal equivalent circuit," *IEEE Trans. Microw. Theory Techn.*, vol. 38, no. 7, pp. 891–895, Jul. 1990.

[13] J. P. Dunsmore, *Handbook of Microwave Component Measurements: With Advanced VNA Techniques*. New York, NY, USA: Wiley, 2012.

[14] P. Colantonio *et al.*, "Improved phase linearity in source field plate AlGaN/GaN HEMTs," in *Proc. 44th Eur. Microw. Conf.*, Oct. 2014, pp. 349–352.

[15] W. Jatal, U. Baumann, K. Tonisch, F. Schwierz, and J. Pezoldt, "High-frequency performance of GaN high-electron mobility transistors on 3C-SiC/Si substrates with Au-free ohmic contacts," *IEEE Electron Device Lett.*, vol. 36, no. 2, pp. 123–125, Feb. 2015.

[16] X. Fu *et al.*, "High-frequency InAlN/GaN HFET with f max over 400 GHz," *Electron. Lett.*, vol. 54, no. 12, pp. 783–785, Jun. 2018.

[17] F. Cozette *et al.*, "Resistive nickel temperature sensor integrated into short-gate length AlGaN/GaN HEMT dedicated to RF applications," *IEEE Electron Device Lett.*, vol. 39, no. 10, pp. 1560–1563, Oct. 2018.